Available online at www.sciencedirect.com
ScienceDirect
Earth and Planetary Science Letters 256 (2007) 278–293
EPSL
www.elsevier.com/locate/epsl

Lithium elemental and isotopic disequilibrium in minerals from peridotite xenoliths from far-east Russia: Product of recent melt/fluid–rock reaction

Roberta L. Rudnick [a,*], Dmitri A. Ionov [b,c,1]

[a] Geochemistry Laboratory, Department of Geology, University of Maryland, College Park, MD 20742, USA
[b] Institut für Mineralogie, J.W. Goethe-Universität, Senckenberganlage 28, 60054 Frankfurt/Main, Germany
[c] Max-Planck-Institut für Chemie, Postfach 3060, D-55020 Mainz, Germany

Received 10 September 2006; received in revised form 26 January 2007; accepted 26 January 2007
Available online 3 February 2007
Editor: R.W. Carlson

Abstract

Lithium concentrations and isotopic compositions of coexisting olivine and clinopyroxene (cpx) in well-characterized peridotite xenoliths from Tok (SE Siberian craton) and samples from two other far-east Russian localities reveal strong elemental and isotopic disequilibria, which correlates with bulk rock composition. Lithium concentrations in cpx from Tok (1–12 ppm) are equal to or significantly greater than those in coexisting olivines (1–5 ppm). The Li-rich cpx show core to rim zoning, indicative of Li infiltration from the grain boundaries. Olivines are generally unzoned, although Li concentrations can vary significantly from grain to grain. $^{ol/cpx}D$ varies from 0.2 to 1.0, which is lower than that expected for equilibrium partitioning ($^{ol/cpx}D_{eq}$=1.1 to 2.0), and reflects preferential Li enrichment in cpx. The Li isotopic compositions of both minerals range far beyond normal mantle δ^7Li of ~ +4±2. δ^7Li_{cpx} (−0.8 to −14.6) is systematically lighter than δ^7Li of coexisting olivine (−1.7 to +11.9), and $\Delta^7Li_{ol\text{-}cpx}$ varies from 2.8 to 22.9‰. The greatest elemental and isotopic disequilibria occur in the most fertile samples (lherzolites) and may reflect longer equilibration times and/or enhanced melt permeability in the more refractory samples. Collectively, these observations suggest that the peridotite minerals experienced Li addition via diffusion from a grain boundary melt or fluid shortly before or coincident with their entrainment into the host basalt (i.e., within tens of thousands of years, based on published diffusion coefficients for Li in cpx at the temperatures of equilibration). This diffusional ingress of Li generated large kinetic isotopic fractionation, leading to unusually light cpx and heavier olivines. Thus, low δ^7Li_{cpx} do not reflect the influence of an exotic mantle component related to crustal recycling.

Keywords: upper mantle; metasomatism; Li diffusion; Li isotopes; isotopic disequlibrium; peridotite xenolith

1. Introduction

Studies of Li and its isotopes (^{6}Li: 7.5% and ^{7}Li: 92.5% atomic abundance) in the solid Earth are rapidly increasing in number, as there is great interest in determining whether the Li isotope system will be

* Corresponding author. Tel.: +1 301 405 1311; fax: +1 301 405 3597.
E-mail address: rudnick@geol.umd.edu (R.L. Rudnick).
[1] Current address: Departement Géologie-Pétrologie-Géochimie, Université Jean Monnet, 23 rue Paul Michelon, 42023 Saint-Etienne, France.

0012-821X/$ - see front matter © 2007 Elsevier B.V. All rights reserved.
doi:10.1016/j.epsl.2007.01.035

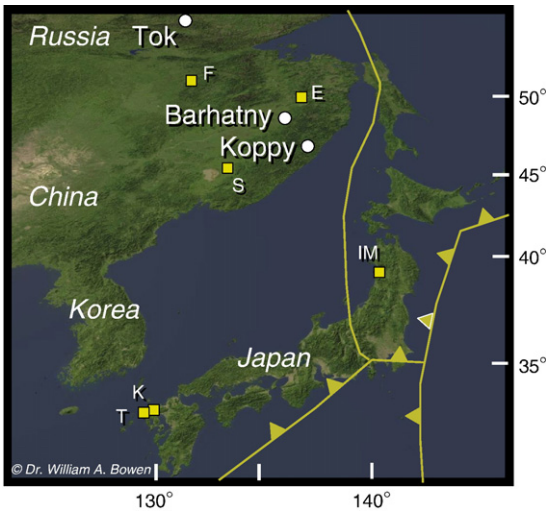

Fig. 1. Map of far-east Russia and vicinity. Circles show xenolith localities investigated here: Tok, Barhatny and Koppy. Whereas Tok occurs within the Precambrian Siberian craton, the latter two localities lie within the Sikhote-Alin Mountains, which run along the eastern seaboard of Russia. Squares are xenolith localities investigated by [29]. F = Fevralsky, E = Ennokentiev, S = Sveyagin, IM = Ichinomegata, T = Takashima and K = Kurose. Cpx from all of the far-east Russian peridotites plus those from Takashima and Kurose have anomalously light δ^7Li. Plate boundaries (subduction zone and transform boundary) are overlain. Latitude and longitude marked in degrees north and east, respectively. Base map courtesy of Dr. William A. Bowen, California Geographical Survey — http://geogdata.csun.edu.

useful for tracing crust–mantle recycling (e.g., [12,38] and references therein). Lithium isotopes can be strongly fractionated at low temperatures, with δ^7Li ($=(^7\mathrm{Li}/^6\mathrm{Li}_{\mathrm{sample}}/^7\mathrm{Li}/^6\mathrm{Li}_{\mathrm{L\text{-}SVEC\ \ standard}}-1)*10^3$) values ranging from +32 in sea water (up to +56 in some sedimentary pore fluids [48]) to very light isotopic compositions in eclogites (≥ -12), which are interpreted as analogs of dehydrated oceanic crust [49]. As for oxygen isotopes, δ^7Li in altered oceanic crust can be either heavy (up to +14) or light (down to −2), depending on the temperature of alteration [2,7,8]. Because Li is a fluid-mobile element ($^{\mathrm{cpx/fluid}}D_{\mathrm{Li}}=0.2$, [4]), it was initially expected that heavy seawater Li incorporated into altered oceanic crust should be removed from the slab during subduction zone metamorphism and follow other fluid-mobile elements into the mantle wedge, ultimately to be sampled again in island arc lavas. However, studies of island arcs show that Li is decoupled from other fluid-mobile elements such as B and Ba, and most island arc lavas have δ^7Li that are indistinguishable from those of MORB ([38], and references therein). Studies of subduction zone metamorphic rocks suggest that δ^7Li may be fractionated during dehydration [49], a supposition supported by recent fluid–pyroxene partitioning data [47]. Thus, the isotopic composition of recycled Li remains a matter of speculation [12].

One way to access the Li isotopic composition of the upper mantle is through the study of peridotite xenoliths, carried in rapidly erupting basalts and kimberlites. Indeed it is through such studies that the composition of the Earth's upper mantle has been defined for major and trace elements [20,27] and for a number of isotopic systems [25,28]. To date, studies of Li isotopes in mantle xenoliths reveal a great range in compositions. The first measurements of whole rock peridotites yielded δ^7Li roughly similar to those of MORB [6,9]. Later studies that focused on mantle xenoliths revealed a more complicated story. Nishio et al. [29] document very large variations in δ^7Li in cpx from mantle xenoliths from far-east Russia and SW Japan. They observed a rough correlation between δ^7Li and Nd and Sr isotopes and suggested that the low δ^7Li reflected a component derived from recycled dehydrated basaltic oceanic crust (EM1, based on Sr and Nd isotopes). In contrast, other studies [21,24,33] find a narrower range of δ^7Li in peridotite xenoliths from a variety of settings (−2 to +4) and, where data exist [33], no correlation between δ^7Li and radiogenic isotope compositions of the cpx.

Here, we report Li concentrations and isotopic compositions of pure olivine and cpx separates from well-characterized and variably (but typically strongly)

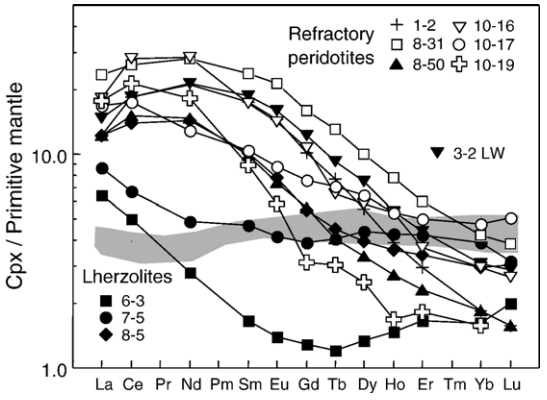

Fig. 2. Primitive mantle-normalized REE patterns of cpx from the Tok xenoliths measured by LA-ICP-MS (data from [15]). LREE-enrichments in the Tok cpx are negatively correlated with modal cpx in the LH series xenoliths [15]. Cpx from refractory peridotites (harzburgites and refractory lherzolites with 3–6% cpx) have strongly enriched LREE and variably depleted HREE. In contrast, cpx from most fertile lherzolites (17% cpx; gray field) have relatively flat patterns at ~5 times primitive mantle. Three moderately refractory lherzolites (10–14% cpx: 6-3, 7-5 and 8-5) show LREE-enrichments. A single wehrlite from the LW series (3-2 LW), for which Li analyses are made, is also shown. Primitive mantle values are from [27].

Table 1
Whole rock and mineralogical characteristics of the samples, including Li concentrations measured by LA-ICP-MS in ppm

Sample No.	Mg#	Cr#	Al_2O_3	Modal abundances, wt.%:				T °C	Li in olivine				Li in opx			Li in cpx			
	Ol	spl	WR	Ol	opx	cpx	phos	Ca-opx	n	Range	Average	σ	n	Average	σ	n	range	Average	σ
Tok: Fertile to moderately refractory spinel lherzolites, lherzolite–harzburgite (LH series)																			
6-1	0.895	0.08	3.94	55	26	17		1010	7	1.8–2.4	2.2	0.2	3†	1.4	0.73	9	1.7–3.3	2.6	0.4
6-2	0.895	0.09	3.98	54	26	17		1001	5	1.9–2.4	2.0	0.2	3†	1.5	1.9	5	2.1–3.0	2.3	0.5
6-3	*0.909*	0.20	2.47	55	33	10		976	6	1.4–2.6	2.0	0.5	4†	2.7	2.4	5	4.0–8.4	5.4	1.7
7-5	0.901	0.12	3.34	57	26	14		985	6	1.3–2.3	1.9	0.4	4	2.2	0.3	10	1.5–5.5	2.9	1.6
8-5	*0.901*	0.14	2.60	63	24	10		1004	9	2.1–5.0	3.4	1.0	2	2.8	0.2	7	1.1–4.8	4.2	0.3
8-6	*0.896*	0.10	3.58	59	23	15		985	9	2.3–3.7	2.9	0.3	1	5.5		8	2.3–9.6	2.6	0.6
8-39	0.894	0.09	3.92	54	26	17		964	9	1.8–2.6	2.2	0.3	1	2.4		8	1.4–2.8	2.4	1.0
Tok: Refractory harzburgites and cpx-poor lherzolites (LH series)																			
1-2	0.913	0.64	0.63	79	17	3	0.1	910	3	4.1–4.2	4.2	0.1	1	2.6		4	2.9–3.8	3.5	0.4
1-3	0.912	0.64	0.70	80	13	5		907	3	4.2–5.0	4.6	0.4	1	3.6		3	9.0–9.9	9.3	0.5
1-13	*0.910*	0.48	0.88	80	16	3		933	3	2.6–3.5	3.1	0.5	1	2.1		1	–	8.2	
2-6	*0.899*	0.44	1.25	67	25	6		980	2	3.5–3.6	3.6		1	5.1		1	–	5.7	
2-9	0.914	0.62	0.76	79	16	3		874	3	2.3–3.7	3.1	0.7	1	0.9		1	–	2.4	
3-4	*0.910*	0.38	1.10	74	21	3		910	2	4.1–4.5	4.3					1	–	5.7	
3-19	*0.900*	0.34	1.30	70	21	6		931	2	2.5–2.7	2.6					3	0.9	0.9	0.0
5-3	0.904	0.27	1.25	74	15	9	0.2	907	4	2.8–3.1	2.9	0.1	2	4.2	0.8	4	1.9–2.5	2.2	0.3
6-0	0.919	0.41	0.79	80	15	3	0.3	890	1	–	2.3								
7-1	0.911	0.55	0.82	79	15	5		985	4	3.3–4.6	3.7	0.7	3	1.8	0.4	4	3.7–4.5	4.2	0.3
8-1	*0.904*	0.27	1.64	74	17	7		1005	3	2.0–2.6	2.3	0.3	3†	1.3	1.0	3†	6.7–13	10.0	2.4
8-2	0.906	0.34	1.26	74	19	6		976	2	3.0	3.0		1	1.8		2	7.9–10	9.0	
8-3	*0.903*	0.46	1.14	74	20	4		956	2	3.6–4.0	3.8		1	2.8	0.2	3	1.4–2.3	1.7	
8-7	0.911	0.55	0.91	77	17	5	0.1	968	4	3.7–4.8	4.3	0.6	1	1.0		2	4.1–7.7	6.0	
8-8	*0.911*	0.47	1.08	72	23	4		955	3	1.7–4.0	3.2	1.2	2	1.3	0.4	3	8.0–9.3	8.6	0.7
8-11	0.913	0.54	0.75	78	17	5		957	3	4.4–4.5	4.4	0.1	3†	4.8	2.5	4	6.0–7.8	6.7	0.9
8-31	0.916	0.56	1.11	76	17	5	0.2	887	3	2.5–3.3	2.9	0.4	2	2.4	0.7	4	5.3–12.4	7.5	3.4
8-50	0.912	0.40	1.14	77	18	4		992	5	1.7–2.4	2.2	0.3	2	1.0	0.1	10	0.5–1.1	0.9	0.2

10-2	0.915	0.59	0.80	77	17	4	0.1	914	2	4.1–4.5	4.3		1	1.8		4	0.5–2.2	1.3	0.7
10-4	0.914	0.57	0.77	80	16	3		926	4	2.2–3.5	2.8	0.6	2	1.4	0.1	5	1.1–2.0	1.6	0.3
10-8	0.908	0.54	0.79	79	15	5		950	3	2.9–3.7	3.2	0.4	1	2.4		3	2.6–2.9	2.7	0.1
10-16	*0.899*	0.51	0.90	76	17	6		957	5	1.8–2.6	2.2	0.3	1	1.3		5	0.8–1.5	1.2	0.3
10-17	0.907	0.24	1.64	76	19	4		1011	7	1.7–2.4	2.2	0.3	1	1.2		5	0.7–1.2	1.0	0.2
10-19	0.911	0.46	0.89	73	23	3	0.3	951	2	1.4–1.7	1.6		1	1.0		5	0.6–1.2	0.9	0.3
Tok: Lherzolite–wehrlite (LW) series peridotites																			
2-1	0.870	0.41	1.59	78	1	19			2	3.3–3.8	3.6					1	–	11.5	
2-2	0.884	0.42	1.59	79	4	14		909	2	2.4–2.5	2.4		1	0.8		1	–	3.0	
2-3	0.884	0.32	1.55	80	5	12		908	2	3.3–4.7	4.0		1	0.9		1	–	3.7	
2-4	0.880	0.31	1.65	80	1	15	0.1		2	3.5–3.9	3.7					1	–	8.4	
2-10	0.882	0.10	3.36	66	11	18		1024	2	3.3–3.8	3.6		1	6.9		1	–	8.7	
3-2	0.890	0.40	1.38	76	6	15		949	4	2.6–3.1	2.8	0.3	2	1.3	0.0	4	1.2–2.2	1.6	0.2
3-22	0.860	0.54	0.98	82	tr.	16	0.1		5	3.1–3.8	3.4	1.8				4	1.7–2.2	2.0	0.3
8-10	0.877	0.26	2.03	79	1	17	0.1	984	5	2.1–3.9	3.0	0.7	2	4.3	0.1	4†	1.1–13.8	7.3	3.7
10-1	0.857	0.14	2.82	71	3	22		964	3	2.3–3.0	2.7	0.4	2	2.3	0.3	7	0.9–3.0	1.7	0.9
10-3	0.842	0.63	0.76	84	tr.	16		982	3	2.9–4.3	3.6	0.7	2	2.0	1.9	4	1.2–2.3	1.6	0.5
10-11	0.851	0.47	0.82	78	13	7	0.4	920	5	4.7–6.3	5.5	0.7	2	4.1	0.6	3†	5.0–11	7.4	3.1
Sikhote-Alin spinel lherzolite xenoliths																			
13-8	0.903	0.15	2.53			10		905	1	–	4.1		1	1.8		2	6.5–29	17.6	
8802-1	0.900	0.11	3.00	65.7	21.5	10		987											

n = number of spot analyses.

Modal, chemical and equilibration temperature (T) data are from Ionov et al. [14–17,19]; Mg# in italics are for heterogeneous olivine.

Ol, olivine; opx, orthopyroxene; cpx, clinopyroxene; phos, phosphates (apatite and whitlockite). T estimates are after Brey and Kohler (1990) [5].

†Pyroxenes with broadly variable Li abundances (>50% difference for duplicate analyses).

Samples shown in bold were measured for lithium isotopes (see Table 2). Sikhote-Alin samples are from the following localities: 13-8: Barhatny, 8802-1 Koppy Lava Field.

Li concentrations (in ppm) of international standards measured by LA-ICP-MS in the same lab include: BHVO-2g=4.47±0.44 (n=8); BCR-2g=9.4±0.24 (n=7); BIR-1g=3.3±0.24 (n=6), GOR132=10.2±0.64 (n=16); BM90/21g=2.19±0.18 (n=7) (all uncertainties are 2σ).

metasomatised peridotite xenoliths from far-east Russia, as well as Li concentrations obtained by laser-ablation inductively coupled mass-spectrometry (LA-ICP-MS) in olivine and pyroxenes from a total of over 40 xenoliths. We use these data to explore the geographic distribution of anomalous Li abundances and isotope compositions in the NE Asian mantle and investigate the origin of the anomalous signatures.

2. Samples

The majority of the xenoliths in this study are from Quaternary (0.3–0.6 Ma) alkali basaltic lavas at Tok in the south-eastern Siberian craton, Russia (Fig. 1). Mineral major and trace element data, thermometry, whole rock major and trace element data, platinum group element concentrations and Sr, Nd, Hf and Os isotope data have previously been reported for these xenoliths by Ionov and coworkers [14,15,17,19]. Ionov et al. [17] identified two main rock series among Tok peridotite xenoliths. Samples in the lherzolite–harzburgite (LH) series range from fertile to highly refractory compositions (4 to 0.6 wt.% Al_2O_3), reflecting variable amounts of melt extraction at shallow levels. Refractory (olivine-rich, cpx-poor), LH peridotites are strongly metasomatised, as indicated by convex-upward trace element patterns (Fig. 2), the presence of accessory minerals (phosphates, alkali feldspar, phlogopite, amphibole) and cryptocrystalline interstitial materials, Na-rich cpx, etc. [15,16]. Minerals in the LH series peridotites are generally homogeneous, although multiple olivine generations are present in some samples (see samples marked by asterisks in Table 1 and [17]). Lherzolite–wehrlite (LW) series rocks were produced by interaction of the LH series protoliths with evolved silicate melts, which partially or completely replaced orthopyroxene (opx) with cpx and caused moderate to strong Fe-enrichments [14]. Li concentrations (Tables 1 and 2) and isotopic compositions were determined for mineral separates (cpx, olivine and, in two samples, opx) in 12 LH series and one LW series xenoliths, as well as the host basalt (Table 2). Li concentrations in coexisting minerals were determined *in situ* for a much larger sample population (Table 1).

The Tok suite has been selected for this study for several reasons. (1) It is located near the subduction-related Pacific margin of Siberia, approximately 400–1000 km north from the far-east Russian localities where Nishio et al. [29] found cpx with anomalous Li-isotope compositions (Fig. 1). (2) Nearly all the Tok xenoliths are metasomatised to various degrees (e.g., most are LREE-enriched, Fig. 2) and many appear to have experienced several metasomatic events [15]. (3) Detailed information about petrography, chemical and isotope composition of the xenoliths is available from earlier [14–17,19] and ongoing [45] work.

Two other xenoliths studied here come from the northern Sikhote-Alin Mountains in far-east Russia (Fig. 1). Sample 13-8 is a metasomatised, feldspar-bearing lherzolite from the Barhatny volcanic center that is strongly LREE-enriched [22]. Sample 8802-1 is a LREE-depleted spinel lherzolite from the Koppy volcanic field close to the Japan Sea coast [18], and hence closest to the subduction zone. The Li concentration and isotopic composition for the Barhatny host basalt is given in Table 2. Essential information on all the samples from this study is summarized in Table 1.

3. Analytical methods

Li concentrations were measured in situ by laser ablation inductively-coupled plasma mass spectrometry (LA-ICP-MS) with a precision and accuracy of $\leq 10\%$. Li concentrations and isotopic compositions for clean mineral separates were measured by the sample-standard bracketing method using a Nu Plasma multi-collector ICP-MS (MC-ICP-MS) following the procedures outlined in Rudnick et al. [32], with a precision of $\leq 1‰$ on δ^7Li and $\pm 15\%$ on Li concentration. Full details of the analytical methods are provided in the electronic supplement.

4. Results

Lithium concentrations of the peridotite minerals determined by LA-ICP-MS are provided in Table 1 and Li concentrations and isotopic compositions determined by MC-ICP-MS are reported in Table 2.

4.1. Heterogeneous Li distribution in minerals and comparison of methods

Analyses of pyroxenes by LA-ICP-MS in some of the Tok peridotites and in the single sample from Barhatny (13-8) can show variations in Li concentrations that are well beyond analytical uncertainty (with % RSD ranging up to 54%, Table 1), indicating significant compositional heterogeneity. In some cases, this heterogeneity can be seen as significant changes in Li/Si or Li/Ca signal ratios within individual pyroxene grains during ablation, while signal intensities for other elements remain constant, indicating zoning in Li but not other elements. The strongest Li zoning and grain-to-grain variations are seen in cpx, followed by opx.

Table 2
Lithium concentrations and isotopic compositions of minerals from peridotite xenoliths from far-east Russia

Sample	Locality	Rock type	Mineral	Handling	Li ppm MC-ICP-MS	Li ppm LA-ICP-MS	1σ	δ^7Li	n	$\Delta^7Li_{ol\text{-}cpx}$	$^{ol\text{-}cpx}D$
Tok: Fertile to moderately refractory spinel lherzolites, lherzolite–harzburgite (LH series)											
6-1	Tok	Lherzolite	cpx	Leached	n.d.			−6.4	1	14.9	0.4
			cpx-r	Leached	4.4			−7.3	2		
			cpx#	Leached	2.1				1		
			cpx ave		**3.3**	2.6	0.4	**−6.9**			
			ol	Washed	1.3	2.2	0.1	8.1	2		
6-3*	Tok	Lherzolite	cpx	Leached	6.7	5.4	1.7	−9.3	3	21.1	0.2
			ol	Washed	1.5	2.0	0.5	11.8	1		
7-5	Tok	Lherzolite	cpx	Leached	4.8	2.9	1.6	−9.8	1	21.7	0.3
			ol	Washed	1.5			11.6	1		
			ol-r	Washed	1.7			12.1	1		
			ol ave		**1.6**	1.9	0.4	**11.9**			
8-5*	Tok	Depl. Lherz	cpx	Leached	4.8			−13.2	2	13.7	0.5
			cpx-r	Leached	3.3			−12.6	2		
			cpx ave		**4.1**	4.2	0.3	**−12.9**			
			ol	Washed	2.2			1.0	3		
			ol-r	Washed	2.1			0.5	1		
			ol ave		**2.1**	3.4	1.0	**0.8**			
8-6*	Tok	Lherzolite	cpx	Washed	3.7			−10.8	2	18.8	0.4
			cpx-r	Washed	4.8			−10.6	2		
			cpx ave		**4.3**	2.6	0.6	**−10.7**			
			opx	Washed	3.2			−11.8	1		
			opx-r	Washed	3.3			−11.8	1		
			opx ave		**3.3**	5.5		**−11.8**			
			ol	Washed	1.3			7.8	1		
			ol#	Leached	1.7			10.1	1		
			ol#	Washed	1.4			6.3	1		
			ol ave		**1.5**	2.9	0.3	**8.1**			
8-39	Tok	Lherzolite	cpx	Washed	4.1			−14.7	3	22.9	0.5
			cpx-r	Washed	1.2			−13.9	2		
			cpx#	Leached	4.4			−15.3	1		
			cpx ave		**3.2**	2.4	1.0	**−14.6**			
			opx	Washed	3.2			−13.2	1		
			opx-r	Washed	3.3			−13.9	1		
			opx ave		**3.3**	2.4		**−13.6**			
			ol	Washed	1.7			8.1	1		
			ol-r	Washed	1.8			8.5	1		
			ol ave		**1.8**	2.2	0.3	**8.3**			
Tok: Refractory harzburgites and cpx-poor lherzolites (LH series)											
1-2	Tok	Harzburgite	cpx	Washed	4.8			−3.0	2	3.6	1.0
			cpx#	Leached	3.9			−3.1	1		
			cpx ave		**4.4**	3.5	0.4	**−3.0**			
			ol	Washed	4.2	4.2	0.1	0.6	1		
8-31	Tok	Harzburgite	cpx	Washed	8.3	7.5	3.4	−7.3	1	9.6	0.4
			ol	Washed	3.0	2.9	0.4	2.3	1		
8-50	Tok	Harzburgite	cpx	Washed	2.1			−8.9	2	7.4	1.0
			cpx-r	Washed	2.4			−9.3	2		
			cpx ave		**2.3**	0.9	0.7	**−9.1**			
			ol	Washed	2.1			−1.0	2		
			ol-r	Washed	2.4			−2.4	2		
			ol ave		**2.3**	2.2	0.3	**−1.7**			
10-16*	Tok	Harzburgite	cpx	Leached	1.6	1.2	0.3				0.7
			ol	Leached	1.1	2.2	0.3	3.3	1		
10-17	Tok	Harzburgite	cpx†	Washed	1.4	1.0	0.2	−1.9	3	4.0	1.1
			ol	Leached	1.5	2.2	0.3	2.1	1		

(continued on next page)

Table 2 (*continued*)

Sample	Locality	Rock type	Mineral	Handling	Li ppm MC-ICP-MS	Li ppm LA-ICP-MS	1σ	δ^7Li	*n*	$\Delta^7Li_{ol\text{-}cpx}$	$^{ol\text{-}cpx}D$
10-19	Tok	Harzburgite	cpx†	Washed	1.2	0.9	0.3	−2.1	3	4.9	1.1
			ol	Leached	1.3	1.6		2.8	1		
Tok: Lherzolite–wehrlite (LW) series peridotites											
3-2	Tok	Wehrlite	cpx	Washed	1.2			−0.7	2	2.8	2.1
			cpx#	Leached	1.9			−0.8	1		
			cpx ave		**1.6**	1.6	0.2	**−0.8**			
			ol	Washed	3.2	2.8	0.3	2.0	1		
Sikhote-Alin spinel lherzolite xenoliths											
13-8	Barhatny	Lherzolite	cpx	Washed	6.6	17.6	–	−6.3	2	11.0	0.7
			ol	Washed	5.0			4.4	1		
			ol-r	Washed	4.5			5.0	1		
			ol ave		**4.8**	4.1	–	**4.7**			
8802-1	Koppy	Lherzolite	cpx	Washed	1.2			3.0	1	1.0	1.3
			ol	Washed	1.5			4.0	1		
Host basalts											
8-1 bas	Tok	Host basalt		None	11.8			1.2	1		
Bh-1	Barhatny	Host basalt		None	7.8			3.4	1		

mineral abbreviations: cpx = clinopyroxene, ol = olivine, -r following mineral symbol indicates replicate analysis, # means replicate dissolution (see text for details).
δ^7Li values are averages of repeat analyses where *n* = number of analyses of particular solution.
*Samples containing heterogeneous olivines according to Ionov et al. (2005) [17].
†Samples analyzed in Frankfurt.
– in 1 sigma column indicates <3 spot analyses, so no standard deviation was calculated.

Reproducibility of the LA-ICP-MS analyses for Li in olivines is generally better than that for the pyroxenes (i.e., RSD for olivines are typically lower than for cpx in individual samples, Table 1), suggesting that olivines have more uniform Li concentrations.

Profiles across cpx from three samples (Fig. 3) show variable, but generally higher Li concentrations on cpx rims in the two lherzolite samples (8-6 and 8-5), and relatively constant Li in the single harzburgite investigated. Li in the lherzolite cpx is enriched by up to a factor of three on rims relative to the cores. Due to the large size (120 μm) of the laser beam used, and because the laser pits are ≥30 μm away from the cpx rims, small-scale Li zoning in the cpx may be even more dramatic. In contrast, profiles across olivines in the same samples show little change in Li content from core to rim (Fig. 3). Nevertheless, different olivine grains in these samples can have significantly different Li contents (e.g., Li contents in olivines from sample 8-5 range from 2 to 5 ppm, Table 1). Thus olivine grains appear to be unzoned, within the limits of the precision of the method, but individual samples may contain different populations of olivines that have distinctive Li concentrations.

Li concentrations in cpx determined by MC-ICP-MS are generally higher than the average of LA-ICP-MS analyses, and for several samples do not fall within analytical precision of the LA-ICP-MS results (see supplemental Fig. S1 in the Appendix). However, in many cases the solution concentrations do overlap the range of concentrations determined by LA-ICP-MS. This general offset in concentrations may reflect a greater proportion of high-Li cpx analyzed by solution. Indeed, laser analyses were performed primarily on clear cpx cores, and most samples contain cloudy cpx rims as well as interstitial cpx, both of which may have higher Li contents. The concentration profiles shown in Fig. 3 confirm that Li is generally enriched on cpx rims in these samples (and micron-scale enrichments can be even greater).

Lithium concentrations determined by the two methods for olivines do not show a very good correlation (supplemental Fig. S1 in the Appendix), particularly at the lowest concentrations, where the laser data generally return higher values than the MC-ICP-MS data. Sample 8-5 shows significant grain-to-grain Li variability in olivine, from 2.1 to 5.0 ppm (Table 1), although the single olivine grain that was profiled revealed no significant core to rim zoning (Fig. 3), suggesting a heterogeneous olivine population with respect to Li concentrations. It is possible that similar inter-grain heterogeneity can explain the differences between olivine Li contents measured by the two methods for sample 8-6, although the nine laser

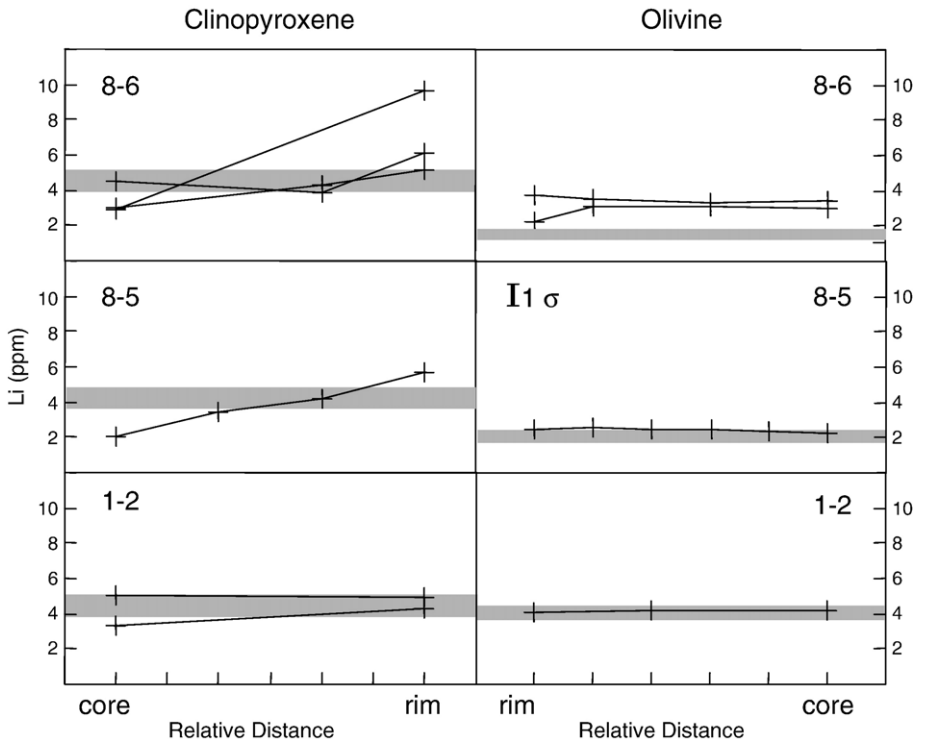

Fig. 3. Zoning profiles through cpx (left panels) and olivines (right panels) from Tok xenoliths. Horizontal scale is arbitrary, but varies from 300 to 800 μm for the cpx and from 700 to 1300 μm for olivine. Laser spot sizes are 120 μm. Analytical uncertainty is shown for each panel. Gray shaded field represents average composition determined by solution ICP-MS; width of bar is ±1 sigma uncertainty (15%). Samples 8-6 and 8-5 are relatively fertile peridotites, whereas sample 1-2 is a refractory harzburgite.

spot analyses do not range below 2.3 ppm (Table 1), compared to a replicated solution concentration of 1.5 ppm (Table 2).

4.2. Li abundances in minerals

Lithium concentrations determined by LA-ICP-MS in olivine from Tok xenoliths are plotted against those in coexisting opx and cpx in Fig. 4. Olivines contain between 1.6 and 5.5 ppm Li, whereas cpx show an even greater range, from 0.9 to 11.5 ppm. The Li concentrations in most olivines and in pyroxenes greatly exceed those reported for fertile spinel and garnet peridotites from elsewhere (oval field in Fig. 4), including mantle xenoliths in basalts from nearby intra-plate localities (Baikal region, Mongolia) [21,24,33,34]. Li abundances in minerals from refractory peridotites show a greater range and tend to be higher than those of the LH series lherzolites. Olivines from the more fertile lherzolites (less than 60% modal olivine) have concentrations overlapping those of the primitive mantle (Fig. 5). In contrast, only a few of the olivines in refractory peridotites have the low Li concentrations expected in olivines of melt extraction residues; most have considerably higher Li contents (Fig. 5).

In a very few LH series peridotites, mainly refractory rocks, both the absolute Li abundances (0.7–2.5 ppm) and the relative abundances between the different mineral phases ($Li_{ol} > Li_{cpx} \geq Li_{opx}$) are similar to those found in "equilibrated" mantle peridotites (i.e., those that do not contain metasomatic minerals and show inter-mineral equilibration of transition metals, [34]) (oval field in Fig. 4). In most cases, however, the relative abundance of Li between olivine and pyroxenes do not match equilibrium values (i.e., $^{ol/cpx}D = 1.1$ to 2.0, [4,11,34]). In nearly all fertile lherzolites and in a majority of the refractory peridotites, Li concentrations in the Tok pyroxenes are much higher than those in olivine and show inverse relative abundances to those observed in "equilibrated" mantle, with $Li_{cpx} > Li_{opx} > Li_{ol}$ (Table 1, Fig. 4). This abundance pattern is similar to those of "unequilibrated" peridotites that are interpreted to have experienced recent metasomatism by mafic silicate melts [30,34,46]. A few refractory peridotites and wehrlites show the inverse, with $^{ol/cpx}D > 2$ (Fig. 4), a pattern previously attributed to carbonatite metasomatism [34,46].

4.3. Li isotopic compositions

The δ^7Li values of both olivines and cpx in the Tok peridotites are highly variable, with cpx consistently having lower δ^7Li than coexisting olivines by 3 to 23‰. Li isotopic compositions of opx from two lherzolites has very light δ^7Li, indistinguishable from that of the coexisting cpx (Table 2). The δ^7Li in olivines range from a low of −2 to a high of +12, straddling the values of upper mantle (+4 ± 2), based on the isotopic compositions of oceanic basalts ([38], and references therein; [39]). In contrast, the δ^7Li of cpx are all very light, ranging from −1 to −15, and are similar to those observed by Nishio et al. [29] for cpx from peridotite xenoliths from other localities from far-east Russia and SW Japan (−3 to −17). The δ^7Li of olivines correlates with modal olivine (hence the degree of melt extraction),

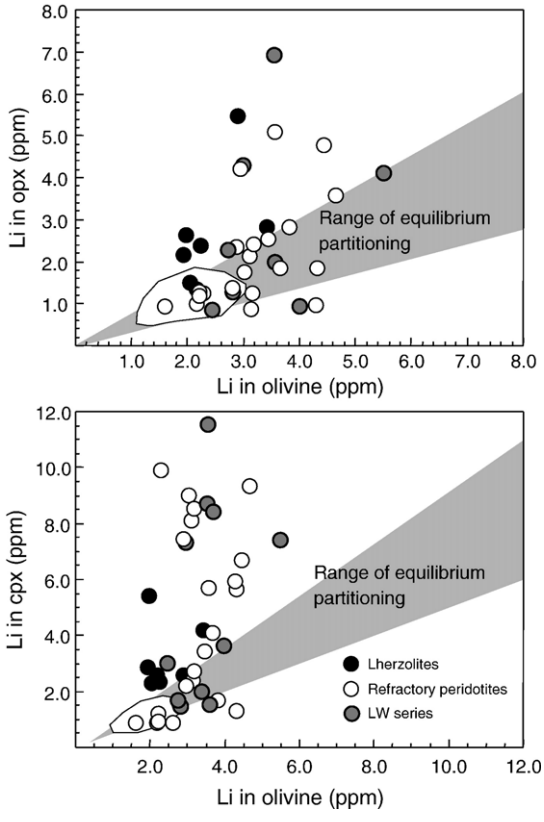

Fig. 4. Lithium concentrations measured by LA-ICP-MS in coexisting minerals from Tok peridotite xenoliths. "Lherzolites" and "Refractory peridotites" constitute the LH series samples mentioned in the text. Gray field represents range of possible equilibrium *D*-values based on experimental data from [4] and subsolidus partitioning relations derived from observations on equilibrated peridotite xenoliths from [11] and [34]. Oval fields enclose range of data for equilibrated peridotites from the literature. Data from Table 1.

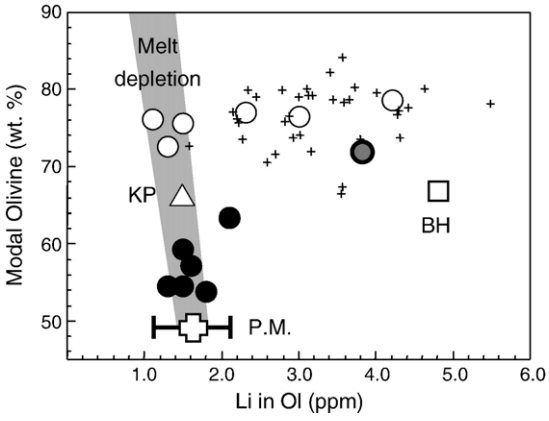

Fig. 5. Lithium concentration in olivine plotted against modal olivine content. Solid and open circles: Tok data measured by MC-ICP-MS. Gray circle is the single wehrlite sample. Open symbols: MC-ICP-MS data from xenoliths from Sikhote-Alin, where BH = Barhatny (square) and KP = Koppy Lava Field (triangle). P.M. is whole rock primitive mantle from [27] (with associated uncertainty). Crosses are Li data measured by LA-ICP-MS for samples where no solution measurements are available. Melt depletion trend (gray field) is based on Li concentrations in refractory peridotites (data from [11,34]) and encompasses a batch melting model, assuming a correlation between modal olivine and Mg# as depicted by [3] and Mg# and Li ppm as depicted by [35].

with more fertile samples having distinctly heavier olivine (Fig. 6a). In contrast, δ^7Li of cpx shows only a poor correlation with modal olivine (Fig. 6b).

The two samples from Sikhote-Alin show contrasting behavior. Whereas olivines in both samples have δ^7Li near average upper mantle (+4.8 and +4.0 in the Barhatny and Koppy samples, respectively, Table 2), their cpx differ greatly. The Barhatny cpx has light δ^7Li (−6.3), within the range of Tok cpx, and the Koppy cpx has a heavier δ^7Li (+3.0), which is the only cpx measured in this study that falls within the range of typical upper mantle.

The offset between δ^7Li in olivine and cpx, described as $\Delta^7\mathrm{Li}_{\text{ol-cpx}}$ ($=\delta^7\mathrm{Li}_{\text{ol}}-\delta^7\mathrm{Li}_{\text{cpx}}$), correlates with both bulk composition and the degree of elemental disequilibrium. Samples with the greatest modal olivine content, i.e., the most refractory samples, have the lowest $\Delta^7\mathrm{Li}_{\text{ol-cpx}}$ (Fig. 7). Similar correlations are observed for other parameters sensitive to the degree of melt extraction, such as bulk rock Al_2O_3 contents, or Cr# of spinel and Mg# of olivine. Collectively, the data plotted in Fig. 7 show that as the cpx becomes progressively more Li-enriched (as reflected by low $^{\text{ol/cpx}}D$), the degree of isotopic disequilibrium (as measured by higher $\Delta^7\mathrm{Li}_{\text{ol-cpx}}$) increases. The single sample from the Koppy Lava Field (KP) shows elemental equilibrium and has $\Delta^7\mathrm{Li}_{\text{ol-cpx}}$ within error of zero, whereas the single measured wehrlite from Tok has a relatively low

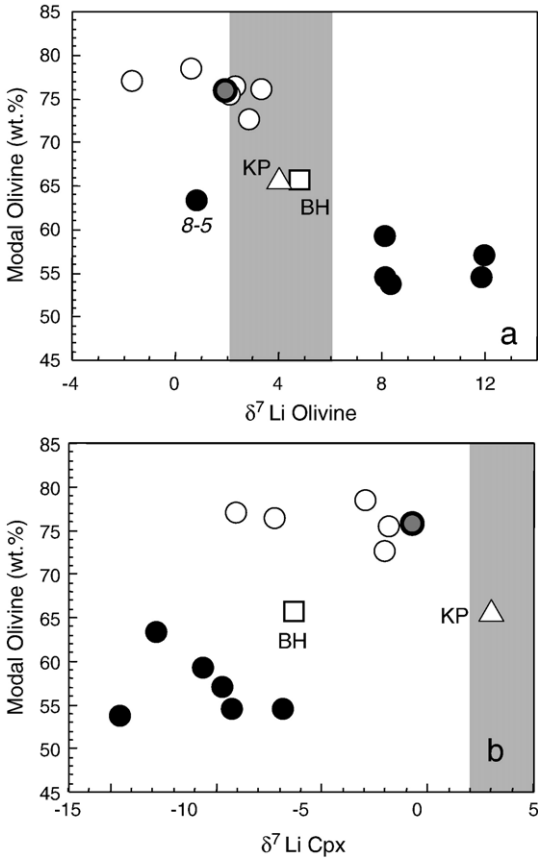

Fig. 6. Lithium isotopic composition (δ^7Li) versus modal olivine (wt.%) for (a) olivines and (b) cpx. Vertical gray bars represent range of δ^7Li of "normal" upper mantle, as deduced from oceanic basalts ([38], and references therein; [39]). Modal olivine from [14,17,18]. Symbols as in Fig. 5.

$\Delta^7Li_{ol\text{-}cpx}$, but has a high $^{ol/cpx}D$. Thus, in this sample, in contrast to nearly all others from Tok, the olivine is enriched in Li relative to the cpx.

5. Discussion

The results presented above demonstrate correlations between Li concentrations, isotopic compositions and modal and chemical compositions for the Tok peridotites that can be used to infer the processes and factors that control the Li isotopic composition of mantle xenoliths. In the following discussion we use experimental and empirical Li partitioning data to evaluate equilibrium Li partitioning between coexisting mantle phases [4,11,34]. Unfortunately, equilibrium Li isotopic fractionation at mantle temperatures is not well constrained, as no experimental data are yet available and empirical studies suggest a rather wide range of possible values for $\Delta^7Li_{ol\text{-}cpx}$ (from −5 to 4, [21,24,33]). Given the absence of Li isotopic fractionation during basalt differentiation [40] and the acknowledgment that arrested high-temperature diffusion may cause significant isotopic fractionation [23,31,37] (which may be especially important in mantle xenoliths that cool rapidly upon ascent, [21,24]), we assume that equilibrium $\Delta^7Li_{ol\text{-}cpx}$ at mantle temperatures is zero.

5.1. Lithium infiltration and disequilibria

The generally high concentrations of Li in olivines, opx and cpx in the Tok and Barhatny xenoliths compared to "normal" mantle (Fig. 4), coupled with the heterogeneous Li concentrations of olivines and cpx and increased Li concentrations observed on the rims of some cpx (Fig. 3) point to recent Li addition to these samples. Lithium diffusion in cpx [10] is orders of magnitude more rapid than for other incompatible trace elements at mantle temperatures [36,42], and, given knowledge of the diffusion coefficient for Li in cpx at the appropriate temperatures, the zoning can be used to determine when the Li was added. Using a diffusion coefficient for Li in cpx between 10^{-13} and 10^{-12} [10] (corresponding to equilibration temperatures in the xenoliths of 900 to 1000 °C, [17]), it would take between 10 and 80 ka for the Li zoning to disappear in a 1 mm wide cpx. If the xenoliths experienced transient heating associated with the infiltration of the Li-rich fluid or melt, which may not be

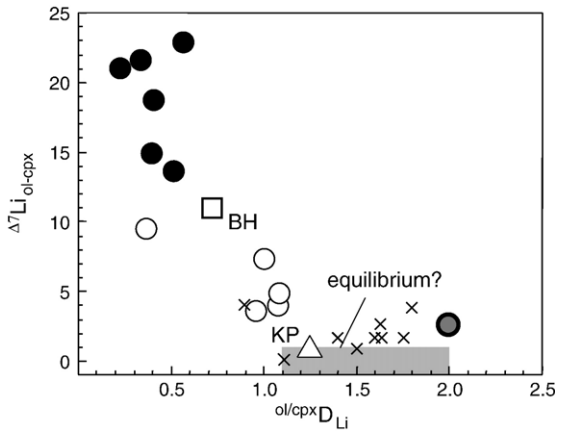

Fig. 7. Partition coefficient for Li between olivine and cpx ($^{ol/cpx}D$, calculated from MC-ICP-MS data) versus the degree of isotopic equilibrium ($\Delta^7Li_{ol\text{-}cpx}$). Gray horizontal bar shows equilibrium conditions (from [4,11,33,34]) with equilibrium $\Delta^7Li_{ol\text{-}cpx}$ assumed here to be zero (±1‰) at mantle temperatures (see text). Crosses are "equilibrated" peridotites from [33]. The trend in the Tok data illustrates that isotopic and elemental disequilibrium are correlated. The single sample from the Koppy Lava Field appears to be fully equilibrated.

reflected in their equilibration temperatures due to more sluggish diffusion of the elements used in thermometry, then the equilibration time is even shorter. Thus, the Li addition must have been a very recent event, occurring within tens of thousands of years before eruption and cooling of the host basalt.

Not only was Li added to the Tok and Barhatny peridotites, but the addition of Li was typically accompanied by the development of strong Li elemental and isotopic disequilibria. In addition to the Li heterogeneity within minerals highlighted above, evidence for disequilibria includes $^{ol/cpx}D$ that are lower than the equilibrium values of 1.1 to 2.0 [4,11,34] (Fig. 7) and $\Delta^7Li_{ol\text{-}cpx}$ (4 to 23‰) that range well beyond those expected for equilibration at mantle temperatures (assumed here to be zero, as discussed above). The correlations between $^{ol/cpx}D$, $\Delta^7Li_{ol\text{-}cpx}$ and bulk composition (Fig. 7), show that as cpx preferentially takes in Li, the degree of isotopic disequilibrium increases, with lherzolites showing greater overall disequilibria than the refractory peridotites. Thus, even though the high Li concentrations of olivines and cpx in many of the harzburgites suggest they experienced greater overall Li addition (Figs. 4 and 5), it appears that the refractory rocks approached equilibrium more closely than the fertile lherzolites. These features may reflect longer equilibration time for the harzburgites, which would allow for greater overall Li diffusion from a grain boundary fluid or melt and a closer approach to equilibration, with or without a greater influx of Li-rich melt or fluid into the harzburgites relative to the lherzolites. Indeed, the single harzburgite for which we have measured Li profiles in olivine and cpx (sample 1-2), has unzoned minerals with high Li concentration (Fig. 3), consistent with longer equilibration time.

Preferential enrichment of incompatible trace elements in refractory peridotites is a phenomenon seen in xenolith suites the world over [13], and is generally attributed to "mantle metasomatism" (i.e., addition of incompatible elements to refractory peridotite residues due to infiltration or exchange with a highly enriched melt or fluid [26], and references therein). The reasons that harzburgites show greater overall enrichment than lherzolites is not clear, but may reflect the enhanced melt permeability of olivine-rich matrices relative to pyroxene-rich matrices [41,43,44]. The Tok peridotites follow this world-wide trend; the most LREE-enriched cpx are found in the harzburgites, whereas the fertile lherzolites have flat to LREE-depleted patterns [15] (Fig. 2). However, Li does not track the other incompatible trace elements. For example, the amount of Li enrichment in the refractory peridotites is highly variable, and some retain the low Li concentrations expected of partial melting residues (Figs. 4 and 5). Thus, Li enrichment does not correlate well with enrichment of other incompatible trace elements (Fig. 8). Moreover, the Li enrichments do not appear to be correlated with the presence of metasomatic accessory minerals (Table 1). For example, Li abundances in both olivine and cpx in refractory harzburgite 10-19 are among the lowest of the suite, yet this sample has several metasomatic cpx generations and the highest modal phosphates (apatite and whitlockite) among the xenoliths in this study [15,16]. So, although Li is clearly enriched in many of the refractory Tok peridotites, the enrichment does not appear to be ubiquitous, nor well correlated with "metasomatism", as defined by modal mineralogy or the degree of enrichment in highly incompatible trace elements.

A corollary of these observations is that Li was added to these samples in an event that was distinct from the metasomatic enrichment events [15] responsible for the incompatible element-enrichment of these samples. This result is not particularly surprising, since the observed Li disequilibria requires Li enrichment to be a recent phenomenon and the diffusivities of other incompatible trace elements (e.g., REE, Hf, Sr) in cpx are several orders of magnitude slower than Li. These rocks simply did not have enough time in the presence of the Li-bearing fluid or melt to take in other elements that this phase may have been carrying. Thus, the vague correlations between δ^7Li_{ol} and Nd isotopes, LREE-enrichment (Fig. 9a,b) and Sr and Hf isotopes in cpx (not shown) are fortuitous, and simply reflect the general incompatible element enriched characteristics and greater Li isotopic equilibrium of the harzburgites

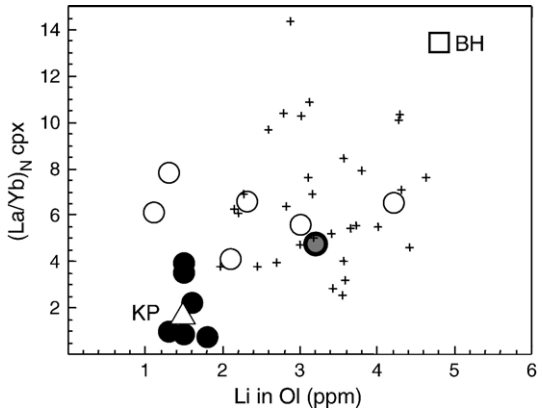

Fig. 8. The concentrations of Li in olivines do not correlate well with the degree of LREE enrichment of the peridotites, as measured by the chondrite-normalized La/Yb ratio of cpx. In particular, the refractory peridotites are all LREE-enriched, but have a large range of Li concentrations. Symbols as in Fig. 5.

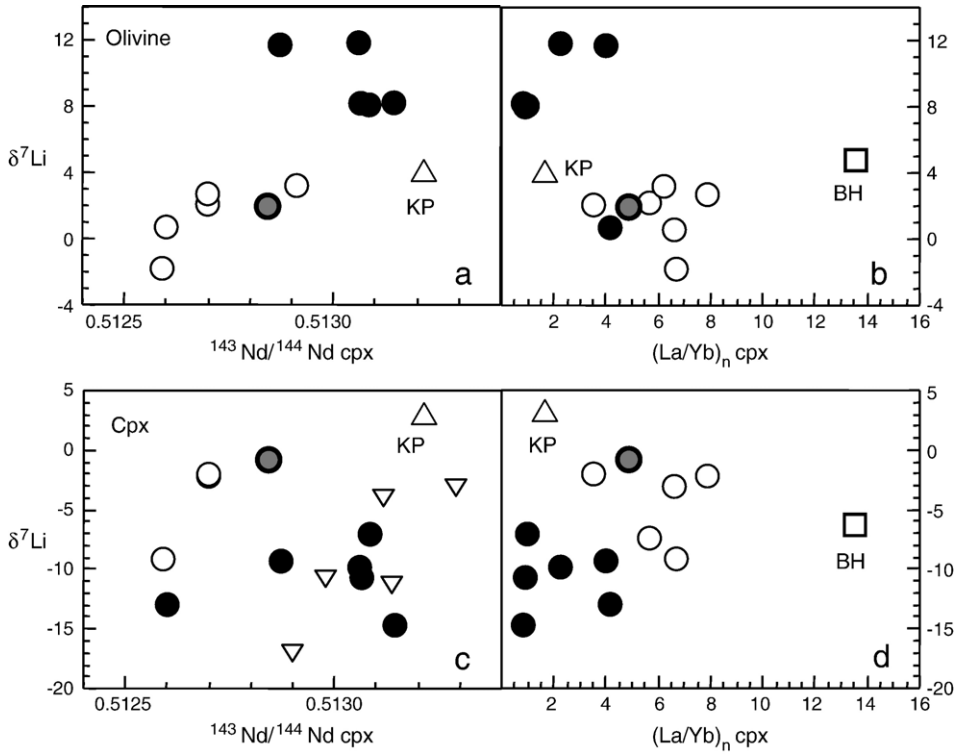

Fig. 9. Lithium isotopic composition of olivine (upper panels) and cpx (lower panels) plotted against degree of incompatible trace element enrichment, as measured by $(La/Yb)_n$ and Nd isotopic composition of cpx. The δ^7Li of olivines correlate with LREE and Nd isotopic enrichment, but those of cpx do not. Similar relationships exist for Sr and Hf isotopes (not shown). Inverted triangles are data for other far-east Russian xenoliths from [29], other symbols as in Fig. 5.

relative to the lherzolites. This interpretation is also consistent with the lack of correlation between δ^7Li_{cpx} and their La/Yb, $^{143}Nd/^{144}Nd$ (Fig. 9c,d) and $^{87}Sr/^{88}Sr$ (not shown).

5.2. Diffusion-induced fractionation of Li isotopes

Recent studies have demonstrated that ^{6}Li diffuses about 2–3% faster than ^{7}Li through melts and minerals [23,31,37]. Modeling of diffusion-induced isotopic fractionation generally assumes diffusional ingress of Li into rocks and minerals from an infinite source of Li, such as Li diffusing into peridotite from a dike of Li-rich basalt [23], or Li diffusing into amphibolite country rocks of a Li-rich pegmatite [37]. As Li diffuses into a substance, an isotopic gradient is established, with the material taking in Li (e.g., mantle minerals, in the case of Li addition to peridotite) first becoming significantly enriched in ^{6}Li, developing low δ^7Li relative to the source of Li, and then finally equilibrating to the $^7Li/^6Li$ ratio dictated by equilibrium partitioning. At high temperatures, where the equilibrium fractionation factor α is expected to be close to 1.00, the δ^7Li of the minerals would eventually adopt that of the source of Li, assuming an infinite reservoir of Li and sufficient time for equilibration.

The marked isotopic disequilibrium of the Tok and Barhatny xenoliths is likely to be a product of such diffusion-driven kinetic isotopic fractionation. In particular, the isotopically light cpx (δ^7Li = −0.8 to −14.6) could be explained by diffusion of Li into the cpx from an infinite source of Li, such as a melt or fluid in an adjacent conduit, whereby the cpx with the lightest Li isotopic composition (generally, those in the fertile lherzolites) occur closest to the source of the Li (see modeling of [23,37]), which show decreases in δ^7Li of up to 20‰ at distances ranging from 1 to 30 m from the contact, depending upon choice of model parameters). However, such an explanation is inconsistent with the isotopically variable, but in some cases very heavy (δ^7Li up to +11.9) compositions of coexisting olivines, since diffusional Li infiltration from such a source should always produce isotopically lighter minerals until equilibration is achieved, at which time the minerals take on the isotopic composition of the Li source. Instead, the large differences in δ^7Li between coexisting cpx and olivine suggest the influence of diffusional processes operating on a much

smaller scale (i.e., from melts/fluids on grain boundaries), with differences between the minerals controlled by the relative diffusivity of Li in cpx versus olivine.

Unfortunately, the diffusion rate of Li in olivine has yet to be measured experimentally, so it is unknown whether Li diffusion in olivine is faster or slower than in cpx at a given temperature. Inferences from natural samples yield conflicting evidence. Jeffcoate et al. [21] observed Li isotopic and elemental zoning in cpx and olivine phenocrysts in a Hawaiian basalt, and suggested that the more pronounced zonation observed in the cpx relative to the olivine reflects faster diffusion of Li into cpx. In contrast, Aulbach et al. [1] found good correlations between δ^7Li_{ol} and Mg# for a suite of mantle xenoliths from Tanzania and no correlation between δ^7Li_{cpx} and Mg#, which they attributed to mixing between a metasomatic melt and the original mantle lithosphere with complete equilibration of the olivine (due to faster diffusion) and lack of equilibration in the cpx. Faster diffusion of Li in olivine relative to cpx could also be inferred by analogy with Mg–Fe and H, all of which diffuse more rapidly in olivine than cpx (see discussion in [1]).

Given the likelihood that diffusion of Li from a grain boundary melt or fluid has produced the observed fractionations in the Tok xenoliths, there may be several ways to explain the observations, including:

1. Li diffusion in olivine is slower than in cpx, and the olivine compositions have not been affected by the recent addition of Li.
2. Li diffusion into olivine is faster than in cpx so that olivines have completely equilibrated with the source of the Li, and the trends seen between δ^7Li_{ol} and bulk rock composition reflect mixing between the original (relatively unmodified) mantle lithosphere and the source of the Li (late stage fluid/melt).
3. The heavy Li in olivine reflects diffusional Li loss from olivine to cpx following metasomatic enrichment, due to inter-mineral re-equilibration driven by changing temperature and/or pressure.
4. Li diffusion in olivine is slower than in cpx and the grain boundary melt or fluid had a very small volume, so that its isotopic composition changed dramatically as Li was lost to diffusional ingress. The melts thus become isotopically heavy as they preferentially lose ^{6}Li and this heavier Li is taken up by the olivines.

Of these possibilities, we believe the last is most likely.

If olivine compositions have been unaffected by Li addition due to slow Li diffusivity in olivine (#1, above), both the elemental and isotopic compositions of the olivines should reflect that of the ambient upper mantle in this region. The highly variable Li concentrations (1–5 ppm) and isotopic compositions of olivines, the high concentrations of Li in many olivines, coupled with the rather extreme isotopic compositions (δ^7Li up to +12) are very different from "normal", equilibrated mantle peridotite [5,21,24,33], and are thus unlikely to represent ambient upper mantle.

On the other hand, if Li diffusivity in olivines is very fast relative to cpx, and the olivines fully equilibrated with the source of the Li to producing mixing trends (#2, above), it is difficult to explain a number of observations, including a) the variable Li concentrations in olivines from a single sample (Table 1) (i.e., they should all have the same concentration since diffusion is so fast), b) the higher Li concentrations in cpx relative to olivine, and c) the very heavy isotopic compositions of olivines in the fertile lherzolites. For example, if this scenario was correct, olivines in the harzburgites that have seen the greatest Li enrichment and more closely approach equilibrium (based on both $^{ol/cpx}D$ and $\Delta^7Li_{ol\text{-}cpx}$) should most closely represent the isotopic composition of the infiltrating melt (in this case, δ^7Li of around −2), and the trend observed between δ^7Li_{ol} and bulk rock composition (Fig. 7) would represent mixing between the original mantle composition (as represented by the fertile lherzolites) and the metasomatic melt (as represented by the harzburgites). The difficulty with this explanation is that the original mantle would have an unusually heavy δ^7Li of +12. For these reasons, we do not favor this hypothesis.

It's also difficult to produce the heavy olivines via inter-mineral diffusion (#3, above). One can produce heavy Li by diffusional loss of Li (since ^{6}Li will leave the mineral first), but the samples that have the heavy olivines also have very low $^{ol/cpx}D$ values, indicating that the cpx have far too much Li to be in equilibrium with olivine, and if anything, Li should diffuse from the cpx into the olivine under these conditions (assuming that $^{ol/cpx}D$ is constant, as suggested by [34]). Thus, there is no reason for Li to diffuse from olivine into cpx.

The most likely explanation for our observations is that the source of Li was a relatively small volume, grain-boundary fluid or melt that was enriched in Li relative to the peridotite (#4, above). As ^{6}Li diffuses preferentially into the peridotite minerals, the remaining fluid/melt becomes isotopically heavier and is taken up by the olivines. If Li diffusion in cpx is faster than in olivine, then the Li entering olivines would consequently be heavier, since light Li is sequestered (temporarily) into the cpx. In contrast, if Li diffusion into olivine is faster

than into cpx, it becomes difficult to explain why $^{ol/cpx}D$ are all very low and why olivine is isotopically heavier. One could argue that the isotopically heavy olivines recrystallized after ^{6}Li was taken into cpx, thereby incorporating heavy, grain-boundary Li into the olivines and leaving the unrecrystallized cpx with isotopically light Li. However, this scenario does not explain the Li enrichment in cpx relative to olivines. Moreover, there is no evidence for late olivine recrystallization in these samples. Thus, we prefer the first hypothesis (faster Li diffusion into cpx).

5.3. Composition and origin of the Li source

Although the source of Li-bearing fluid or melt that infiltrated these rocks cannot be definitively established at this stage, given the evidence that Li enrichment occurred shortly before or during the entrainment of the xenoliths, it is likely to have been a fluid or melt associated with the same phase of alkali basaltic magmatism that gave rise to the host basalts. Petrographic data provide ample evidence for infiltration of a fluid into the Tok mantle shortly before or during the transport of the xenoliths to the surface. For example, the majority of Tok peridotites contain irregularly shaped empty interstitial cavities lined with fine-grained, second-generation olivine, spinel and cpx [17]. Some refractory Tok peridotites also contain quenched interstitial materials enriched in highly incompatible elements [15]. It is likely that the late-stage infiltration of the Li-rich fluid inferred in this paper can be directly linked to the processes recorded in these phenomena. Moreover, abundant cumulate xenoliths with quenched magmatic products are also found at Tok, and some of the LW and LH series peridotites are cut by quenched magmatic veins [14]. Thus, there is evidence for widespread magmatic activity in the Tok mantle shortly before the xenoliths were carried to the surface; degassing and fractional crystallization of those magmas could produce evolved, Li-rich late-stage fluids.

The Li isotopic disequilibrium manifest in the Tok peridotites makes it difficult to infer the isotopic composition of the Li-rich source (as discussed above), but some limits can be had. For this purpose, we focus on the sample that experienced greatest Li addition (so that the Li content of the sample will be swamped by the added Li) and the closest approach to equilibrium, thus minimizing uncertainties related to modal abundances, mineral zoning and grain boundary Li. This sample, refractory harzburgite 1–2, has the highest Li concentration in olivine (4.2 ppm) and the smallest $\Delta^7Li_{ol\text{-}cpx}$ (3.6) of the entire suite. Calculation of the whole rock δ^7Li from mass balance yields +0.1 to +0.5 (depending on whether the opx is assumed to have the same δ^7Li as the cpx, as measured in two other samples, Table 2, or has δ^7Li matching that of the olivine). This composition, while on the light end of δ^7Li seen in typical oceanic basalts [38,39], is indistinguishable from the composition of the host lava (+1.2, Table 2) and is consistent with the Li being added very recently, either shortly before, or possibly even during, xenolith entrainment into the host.

In summary, even though δ^7Li_{cpx} range down to values as low as −15 and δ^7Li_{ol} up to +12, these reflect kinetic isotopic fractionation of Li added to the peridotites shortly before or during their entrainment, and there is no reason to call upon an isotopically light component (δ^7Li<−17), derived from paleo-Pacific subduction (cf., [29]), to explain these unusual isotopic compositions. Indeed, the single peridotite from the Koppy locality, which is closest to the convergent margin boundary (Fig. 1) and consequently might be expected to show the greatest influence of any subduction-derived Li, has a "normal" Li isotopic composition of +3.5 (Table 2).

6. Conclusions

Peridotite xenoliths from the Tok and Barhatny localities in far-east Russia are characterized by strong Li elemental and isotopic disequilibria caused by addition of Li to the rocks via diffusion from a small-volume grain boundary fluid or melt. Because Li diffuses rapidly at mantle temperatures, the disequilibrium is a transient feature and its preservation in these samples indicates that Li addition occurred shortly before or even during the entrainment of the xenoliths in the host basalts. δ^7Li_{cpx} is consistently lower than that of coexisting olivine and $\Delta^7Li_{ol\text{-}cpx}$ correlates with modal and chemical composition of the peridotites. The most refractory samples experienced the greatest overall Li addition and most closely approximate elemental and isotopic equilibrium due to longer equilibration times and probably also greater infiltration of the Li-bearing melt or fluid. The variable but often extreme isotopic compositions produced by this process (δ^7Li_{cpx} down to −15 and δ^7Li_{ol} up to +12) do not reflect the presence of an isotopically exotic recycled component, as has been previously inferred for xenoliths from this region. The best estimate for the δ^7Li of the source of the Li in the Tok xenoliths is δ^7Li=~+0.3, which is indistinguishable from that of the host basalt. A single sample from the Koppy locality, which is situated closest to the paleo-Pacific subduction zone, shows both elemental and isotopic equilibration of Li and has a "normal" δ^7Li

of +3.5. This study highlights the very large isotopic effects that can be produced via kinetic fractionation in peridotite xenoliths at high temperatures and associated with host magma–xenolith interactions.

Acknowledgements

This research was supported by the NSF (EAR0208012 and EAR0609689 to RLR). We thank Emily Baker and Jonathan James for assistance with the mineral separations and Elena Chung for help in carrying out Li column chemistry. DAI thanks A. Hofmann and G. Brey for the support in Mainz and Frankfurt and acknowledges a visiting researcher position at MPI für Chemie in Mainz and a DFG Mercator visiting professorship (Frankfurt); B. Stoll, M. Willbold and Y. Lahaye provided assistance with LA-ICP-MS analyses, S. Durali and M. Seitz helped with analyses of two samples at Frankfurt. Discussions with S. Aulbach, W.F. McDonough, M. Seitz and F.-Z. Teng helped us develop the ideas presented here. We gratefully acknowledge the comments of M. Seitz, T. Elliott, R. Carlson and C. Lundstrom, which helped us to improve the presentation.

Appendix A. Supplementary data

Supplementary data associated with this article can be found, in the online version, at doi:10.1016/j.epsl.2007.01.035.

References

[1] S. Aulbach, R.L. Rudnick, W.F. McDonough, Li–Sr–Nd isotope signatures of the plume and cratonic lithospheric mantle beneath the margin of the rifted Tanzanian craton (Labait), Contrib. Mineral. Petrol. (2007) (in revision).

[2] C. Bouman, T. Elliott, P.Z. Vroon, Lithium inputs to subduction zones, Chem. Geol. 212 (2004) 59–79.

[3] F.R. Boyd, Compositional distinction between oceanic and cratonic lithosphere, Earth Planet. Sci. Lett. 96 (1989) 15–26.

[4] J.M. Brenan, E. Neroda, C.C. Lundstrom, H.F. Shaw, F.J. Ryerson, D.L. Phinney, Behaviour of boron, beryllium, and lithium during melting and crystallization: constraints from mineral–melt partitioning experiments, Geochim. Cosmochim. Acta 62 (12) (1998) 2129–2141.

[5] G.P. Brey, T. Köhler, Geothermobarometry in four-phase lherzolites II. New thermobarometers, and practical assessment of existing thermobarometers, J. Petrol. 31 (1990) 1353–1378.

[6] R.A. Brooker, R.H. James, J.D. Blundy, Trace elements and Li isotope systematics in Zabargad peridotites: evidence of ancient subduction processes in the Red Sea mantle, Chem. Geol. 212 (1–2) (2004) 179–204.

[7] L.H. Chan, J.C. Alt, D.A.H. Teagle, Lithium and lithium isotope profiles through the upper oceanic crust: a study of seawater–basalt exchange at ODP Sites 504B and 896A, Earth Planet. Sci. Lett. 201 (1) (2002) 187–201.

[8] L.H. Chan, J.M. Edmond, G. Thompson, K. Gillis, Lithium isotopic composition of submarine basalts — implications for the lithium cycle in the oceans, Earth Planet. Sci. Lett. 108 (1–3) (1992) 151–160.

[9] L.H. Chan, W.P. Leeman, C.F. You, Lithium isotopic composition of Central American volcanic arc lavas: implications for modification of subarc mantle by slab-derived fluids: correction, Chem. Geol. 182 (2–4) (2002) 293–300.

[10] L.A. Coogan, S.A. Kasemann, S. Chackraoborty, Rates of hydrothermal cooling of new oceanic upper crust derived from lithium-geospeedometry, Earth Planet. Sci. Lett. 240 (2) (2005) 415–424.

[11] S.M. Eggins, R.L. Rudnick, W.F. McDonough, The composition of peridotites and their minerals: a laser-ablation ICP-MS study, Earth Planet. Sci. Lett. 154 (1998) 53–71.

[12] T. Elliott, A. Jeffcoate, C. Bouman, The terrestrial Li isotope cycle: light-weight constraints on mantle convection, Earth Planet. Sci. Lett. 220 (3–4) (2004) 231–245.

[13] F.A. Frey, D.H. Green, The mineralogy, geochemistry and origin of lherzolite inclusions in Victorian basanites, Geochim. Cosmochim. Acta 38 (1974) 1023–1059.

[14] D.A. Ionov, I. Chanefo, J.L. Bodinier, Origin of Fe-rich lherzolites and wehrlites from Tok, SE Siberia by reactive melt percolation in refractory mantle peridotites, Contrib. Mineral. Petrol. 150 (3) (2005) 335–353.

[15] D.A. Ionov, G. Chazot, C. Chauvel, C. Merlet, J.L. Bodinier, Trace element distribution in peridotite xenoliths from Tok, SE Siberian craton: a record of pervasive, multi-stage metasomatism in shallow refractory mantle, Geochim. Cosmochim. Acta 70 (5) (2006) 1231–1260.

[16] D.A. Ionov, A.W. Hofmann, C. Merlet, A.A. Gurenko, E. Hellebrand, G. Montagnac, P. Gillet, V.S. Prikhodko, Discovery of whitlockite in mantle xenoliths: inferences for water- and halogen-poor fluids and trace element residence in the terrestrial upper mantle, Earth Planet. Sci. Lett. 244 (1–2) (2006) 201–217.

[17] D.A. Ionov, V.S. Prikhodko, J.L. Bodinier, A.V. Sobolev, D. Weis, Lithospheric mantle beneath the south-eastern Siberian craton: petrology of peridotite xenoliths in basalts from the Tokinsky Stanovik, Contrib. Mineral. Petrol. 149 (6) (2005) 647–665.

[18] D.A. Ionov, V.S. Prikhodko, S.Y. Oreilly, Peridotite xenoliths in alkali basalts from the Sikhote-Alin, Southeastern Siberia, Russia— trace-element signatures of mantle beneath a convergent continental-margin, Chem. Geol. 120 (3–4) (1995) 275–294.

[19] D.A. Ionov, S.B. Shirey, D. Weis, G. Brügmann, Os–Hf–Sr–Nd isotope and PGE systematics of spinel peridotite xenoliths from Tok, SE Siberian craton: effects of pervasive metasomatism in shallow refractory mantle, Earth Planet. Sci. Lett. 241 (1–2) (2006) 47–64.

[20] E. Jagoutz, H. Palme, H. Baddenhausen, K. Blum, M. Cendales, G. Dreibus, B. Spettel, V. Lorenz, H. Wänke, The abundances of major, minor and trace elements in the earth's mantle as derived from primitive ultramafic nodules, Proc. Lunar Planet. Sci. Conf. 10th (1979) 2031–2050.

[21] A. Jeffcoate, T. Elliott, S.A. Kasemann, D. Ionov, K. Cooper, R. Brooker, Li isotope fractionation in peridotites and mafic melts, Geochim. Cosmochim. Acta 71 (2007) 202–218.

[22] F. Kalfoun, D. Ionov, C. Merlet, HFSE residence and Nb/Ta ratios in metasomatised, rutile-bearing mantle peridotites, Earth Planet. Sci. Lett. 199 (1–2) (2002) 49–65.

[23] C.C. Lundstrom, M. Chaussidon, A.T. Hsui, P. Kelemen, M. Zimmerman, Observations of Li isotopic variations in the Trinity Ophiolite: evidence for isotopic fractionation by diffusion

during mantle melting, Geochim. Cosmochim. Acta 69 (3) (2005) 735–751.
[24] T. Magna, U. Wiechert, A.N. Halliday, New constraints on the lithium isotope compositions of the Moon and terrestrial planets, Earth Planet. Sci. Lett. 243 (3–4) (2006) 336–353.
[25] D.P. Mattey, D. Lowry, C.G. Macpherson, Oxygen isotope composition of mantle peridotite, Earth Planet. Sci. Lett. 128 (3–4) (1994) 231–241.
[26] W.F. McDonough, F.A. Frey, Rare earth elements in upper mantle rocks, in: B.R. Lipin, G.A. McKay (Eds.), Geochemistry and Mineralogy of Rare Earth Elements, vol. 21, Mineralogical Society of America, 1989, pp. 99–145.
[27] W.F. McDonough, S.-s. Sun, Composition of the earth, Chem. Geol. 120 (1995) 223–253.
[28] T. Meisel, R.J. Walker, J.W. Morgan, The osmium isotopic composition of the Earth's primitive upper mantle, Nature 383 (1996) 517–520.
[29] Y. Nishio, S. Nakai, J. Yamamoto, H. Sumino, Y. Matsumoto, V.S. Prikhod'ko, S. Arai, Lithium isotopic systematics of the mantle-derived ultramafic xenoliths: implications for EM1 origin, Earth Planet. Sci. Lett. 217 (2004) 245–261.
[30] L. Ottolini, B. Le Fevre, R. Vannucci, Direct assessment of mantle boron and lithium contents and distribution by SIMS analyses of peridotite minerals, Earth Planet. Sci. Lett. 228 (1–2) (2004) 19–36.
[31] F.M. Richter, A.M. Davis, D.J. DePaolo, E.B. Watson, Isotope fractionation by chemical diffusion between molten basalt and rhyolite, Geochim. Cosmochim. Acta 67 (20) (2003) 3905–3923.
[32] R.L. Rudnick, P.B. Tomascak, H.B. Njo, L.R. Gardner, Extreme lithium isotopic fractionation during continental weathering revealed in saprolites from South Carolina, Chem. Geol. 212 (2004) 45–57.
[33] H.-M. Seitz, G.P. Brey, Y. Layhaye, S. Durali, S. Weyer, Lithium isotopic signatures of peridotite xenoliths and isotopic fractionation at high temperature between olivine and pyroxenes, Chem. Geol. 212 (2004) 163–177.
[34] H.-M. Seitz, A.B. Woodland, The distribution of lithium in peridotitic and pyroxenitic mantle lithologies — an indicator of magmatic and metasomatic processes, Chem. Geol. 166 (1–2) (2000) 47–64.
[35] H.M. Seitz, G.P. Brey, T. Stachel, J.W. Harris, Li abundances in inclusions in diamonds from the upper and lower mantle, Chem. Geol. 201 (3–4) (2003) 307–318.
[36] M. Sneeringer, S.R. Hart, N. Shimizu, Strontium and samarium diffusion in diopside, Geochim. Cosmochim. Acta 48 (1984) 1589–1608.
[37] F. Teng, W.F. McDonough, R.L. Rudnick, R.J. Walker, Diffusion-driven extreme lithium isotope fractionation in country rocks of the Tin Mountain pegmatite, Earth Planet. Sci. Lett. 243 (3–4) (2006) 701–710.
[38] P.B. Tomascak, Developments in the understanding and application of lithium isotopes in the Earth and planetary sciences, in: C. Johnson, B. Beard, F. Albarede (Eds.), Geochemistry of non-traditional stable isotopes, vol. 55, Mineralogical Society of America, Washington, DC, 2004, pp. 153–195.
[39] P.B. Tomascak, C.H. Langmuir, P.J. le Roux, S.B. Shirey, Lithium isotopes in global mid-ocean ridge basalts. Geochim. Cosmochim. Acta (2007) (in revision).
[40] P.B. Tomascak, F. Tera, R.T. Helz, R.J. Walker, The absence of lithium isotope fractionation during basalt differentiation: new measurements by multicollector sector ICP-MS, Geochim. Cosmochim. Acta 63 (6) (1999) 907–910.
[41] A. Toramaru, N. Fujii, Connectivity of melt phase in a partially molten peridotite, J. Geophys. Res., [Solid Earth and Planets] 91 (B9) (1986) 9239–9252.
[42] J.A. Van Orman, T.L. Grove, N. Shimizu, Rare earth element diffusion in diopside: influence of temperature, pressure, and ionic radius, and an elastic model for diffusion in silicates, Contrib. Mineral. Petrol. 141 (6) (2001) 687–703.
[43] N. von Bargen, H.S. Waff, Permeabilities, interfacial areas, and curvatures of partially molten systems: results of numerical computations of equilibrium microstructures, J. Geophys. Res. 91 (1986) 9261–9276.
[44] N. von Bargen, H.S. Waff, Wetting of enstatite by basaltic melt at 1350 °C and 1.0 to 2.5 GPa pressure, J. Geophys. Res. 93 (1988) 1153–1158.
[45] S. Weyer, D.A. Ionov, E. Hellebrand, A.B. Woodland, G.P. Brey, Iron isotope fractionation as indicator of mantle processes, Geochim. Cosmochim. Acta 70 (2006) A697.
[46] A.B. Woodland, H.M. Seitz, G.M. Yaxley, Varying behaviour of Li in metasomatised spinel peridotite xenoliths from western Victoria, Australia, Lithos 75 (1–2) (2004) 55–66.
[47] B. Wunder, A. Meixner, R.L. Romer, W. Heinrich, Temperature-dependent isotopic fractionation of lithium between clinopyroxene and high-pressure hydrous fluids, Contrib. Mineral. Petrol. 151 (2006) 112–120.
[48] C.F. You, L.H. Chan, J.M. Gieskes, G.P. Klinkhammer, Seawater intrusion through the oceanic crust and carbonate sediment in the equatorial Pacific: lithium abundance and isotopic evidence, Geophys. Res. Lett. 30 (21) (2003) 2120, doi:10.1029/2003GL018412.
[49] T. Zack, P.B. Tomascak, R.L. Rudnick, C. Dalpe, W.F. McDonough, Extremely light Li in orogenic eclogites: the role of isotope fractionation during dehydration in subducted oceanic crust, Earth Planet. Sci. Lett. 208 (3–4) (2003) 279–290.

Details of Analytical Methods

Li abundances in olivine, cpx and orthopyroxene (opx) from over 40 xenoliths were determined by LA-ICP-MS in polished grain mounts and 150 μm-thick polished sections (mineral profiles) using a Finnigan Element-2 magnetic sector ICP-MS at MPI für Chemie in Mainz and at Institut für Mineralogie (J.W. Goethe-Universität, Frankfurt/Main), both of which are coupled with automated UP-213 Nd-YAG lasers. The analyses were performed in low-resolution mode using either ^{43}Ca (for cpx) or ^{29}Si (olivine and opx) as internal standards and SRM NIST 612 for external calibration. Reference samples BCR-2g, BHVO-2g, GOR-132 and BM90/21-g were analyzed as unknowns for quality control (Table 1, footnote). Some olivines and opx were analyzed at Frankfurt using both ^{29}Si and ^{25}Mg as internal standards (^{25}Mg yields a high signal-to-background ratio, ~5000:1), using BCR-2g for external calibration and BHVO-2g for quality control; results on duplicate samples were similar to those obtained with NIST 612. All Li concentrations from LA-ICPMS are averages of those measured for ^{6}Li and ^{7}Li isotopes; they are normally within 10% of each other at <5 ppm (see Table S1). The background for ^{6}Li and ^{7}Li was typically 140-200 and 1000-1400 counts per second (cps), respectively, with signal at 2-2.5 ppm level (e.g., BM90/21 or olivine 8-5; Table S1, Fig. 3) of 1200-1400 cpx for ^{6}Li and 9000-16000 cps for ^{7}Li. Typical minimum detection limits (99% confidence) are 0.1-0.15 ppm and 0.05 ppm for ^{6}Li and ^{7}Li, respectively, with 1 sigma error of 0.05-0.20 ppm at 2-5 ppm Li. Reproducibility of Li concentrations for international standards was normally within ±10% (2 σ) at 2-10 ppm Li (Table 1, footnote). Accuracy is also within ±10%, based on comparisons between the standard analyses and nominal values from the literature.

Crushed rocks were sieved to mineral grain size fractions of 300-600 μm that were magnetically separated to obtain olivine- opx- and cpx-rich fractions; minerals were hand picked from the latter to >99% purity. Care was taken to avoid altered grains, or inclusions of or intergrowths with other minerals. Separates were then either washed in an ultrasonic bath of Milli-Q® water (18.2 MΩ cm, three times, for 15 minutes per wash), or were acid leached (first in 10% HF for several minutes, then in warm 10-20% HCl for 30 minutes). Two samples were processed using both purification methods (i.e., leaching and Milli-Q washing) in order to determine whether leaching changes Li concentration or isotopic composition of the separates. The cleaned separates were then crushed by hand in ethanol in an agate mortar and pestle in order to aid digestion, and the powder was dried under a heat lamp.

Sample dissolution and Li purification were achieved following the methods outlined in Rudnick et al. (2004). In order to monitor Li yield, before and after cuts (2 ml each) were analyzed for their Li content using an Element 2, single collector ICP-MS (see below). The total Li procedural blank during the course of this study was ~ 170 pg Li and has a δ^7Li value of -32‰, which represents combined procedural and instrumental blank. This blank is negligible compared to the amount of Li processed for the samples (generally > 50 ng), and given a precision of ±1‰, 2 σ. Thus, no blank corrections were made.

All but two analyses (cpx in 10-17 and 10-19) were performed at the University of Maryland Geochemistry Laboratory where Li isotope measurements were carried out on a Nu Plasma MC-ICP-MS, using the standard bracketing method described in Teng et al. (2004). Prior to analysis, the Na/Li voltage ratio for each solution was measured, as

ratios greater then about 5 cause unstable instrumental fractionations, inhibiting accurate Li isotope determinations (TOMASCAK et al., 1999). In most samples, the Na/Li ratios were suitable for analysis after column chemistry. However, in some cases, high Na/Li ratios were observed, and a second purification through the third column was necessary. Two pure Li standards were routinely analyzed during each analytical session: the in-house standard UMD-1, which is a purified Li solution from Alfar Aesar® and IRMM-016 (Qi et al., 1997). All Li isotope results are given in the δ^7Li notation with $\delta^7\text{Li} = 1000 \bullet [^7\text{Li}/^6\text{Li}_{sample}/^7\text{Li}/^6\text{Li}_{standard}\text{-}1]$ relative to the L-SVEC standard (Flesch et al., 1973) and are calculated by comparison of the unknown sample to the mean of the two bracketing standard analyses, as described in Tomascak et al. (1999b). For two blocks of 20 ratios each, the in-run precision of $^7\text{Li}/^6\text{Li}$ measurements is generally ±0.2‰ or better, with no systematic change in the $^7\text{Li}/^6\text{Li}$ ratio. The external precision, based on repeat runs of Li standard solutions, is ±1‰ (2 σ) or better. During the course of this study UMD-1 and IRMM-016 yielded δ^7Li values of +54.2 ± 1.1 (2 sigma, n=28) and -0.4 ± 1.1 (2 sigma n=19), respectively. The lithium isotopic compositions for a variety of international rock standards ranging in composition from basalt to peridotite (BCR-1, BHVO-1, BIR-1, JB-2, UB-N) and analyzed during the course of this study, are reported elsewhere (AULBACH et al., 2007; RUDNICK et al., 2004; TENG et al., 2006). These standards yield δ^7Li within the range previously reported in the literature.

Because large Li isotope fractionation occurs during ion-exchange chromatography, monitoring the Li yield from column chemistry by measuring before and after cuts is an important tool in evaluating the quality of the Li isotope data (cf. CHAN et al., 2002). Marks et al. (2006) demonstrated that loss of up to 5% total Li during cation exchange

purification produced negligible change in Li isotopic composition. Accordingly, analyses were rejected if more than 5% of the total Li was lost during column chemistry, which occurred in <6% of sample aliquots.

For several samples, two aliquots of dissolved mineral stock solution were processed through the ion-exchange columns as an additional test of the reproducibility of the method (samples designated with an "r" suffix in Table 2). In all cases, these replicates reproduced within the ±1‰ external uncertainty. In addition to replicates, we also performed repeat dissolutions for two separate mineral aliquots from two samples that had been pre-cleaned by acid leaching and washing in Milli-Q. These repeat dissolutions are marked by a hatch mark after the mineral symbol in Table 2. There is no significant difference in Li isotopic compositions between the two pre-cleaning treatments, nor in the Li concentrations. Where replicates are available, the mean Li isotopic composition of the replicates is used as the "true" value.

Li concentrations were determined by comparing the voltage obtained for the sample with that of the two bracketing L-SVEC standards of known concentration, and then adjusting for the sample weight. Uncertainty in the concentrations determined by this method is normally ±10% (Teng et al., 2004). Concentrations for olivines analyzed here replicate to within 15%. Much poorer reproducibility for cpx concentrations (between 13 and 109%) likely reflects heterogeneity of the cpx as seen in LA-ICP-MS analyses and discussed below.

Cpx from two harzburgites (samples 10-17 and 10-19) were measured at the Goethe Universität, Frankfurt/Main. Pure cpx separates (~20 mg) were washed for 60 min in Milli-Q® water and dissolved in an 1:1 HF-HNO_3 mixture. Dried samples were

taken up in 0.18 ml 5 M HNO_3 and 0.72 ml methanol was added. Li was separated on a single 1.4-ml exchange column. Li isotope compositions were measured on a Neptune (ThermoElectron) MC-ICP-MS instrument following procedures similar to those used at the University of Maryland. Details of the analytical methods are given in (SEITZ et al., 2004).

Aulbach S., Rudnick R. L., and McDonough W. F. (2007) Li-Sr-Nd isotope signatures of the plume and cratonic lithospheric mantle beneath the margin of the rifted Tanzanian craton (Labait). *Contrib. Mineral. Petrol.*, (in review).

Chan L. H., Leeman W. P., and You C. F. (2002) Lithium isotopic composition of Central American volcanic arc lavas: implications for modification of subarc mantle by slab- derived fluids: correction. *Chemical Geology* **182**(2-4), 293-300.

Marks M., Rudnick R. L., McCammon C., Vennemann T., and Markl G. (2006) The behavior of Li and its isotopes during igneous fractionation: a case study from the peralkaline Ilímaussaq igneous complex, south Greenland. *Geochimica et Cosmochimica Acta*, (in review).

Rudnick R. L., Tomascak P. B., Njo H. B., and Gardner L. R. (2004) Extreme lithium isotopic fractionation during continental weathering revealed in saprolites from South Carolina. *Chem. Geol.* **212**, 45-57.

Seitz H.-M., Brey G. P., Layhaye Y., Durali S., and Weyer S. (2004) Lithium isotopic signatures of peridotite xenoliths and isotopic fractionation at high temperature between olivine and pyroxenes. *Chemical Geology* **212**, 163-177.

Teng F., McDonough W. F., Rudnick R. L., and Walker R. J. (2006) Diffusion-driven extreme lithium isotope fractionation in country rocks of the Tin Mountain pegmatite. *Earth and Planetary Science Letters* **243**(3-4), 701-710.

Teng F. Z., McDonough W. F., Rudnick R. L., Dalpe C., Tomascak P. B., Chappell B. W., and Gao S. (2004) Lithium isotopic composition and concentration of the upper continental crust. *Geochimica Et Cosmochimica Acta* **68**(20), 4167-4178.

Tomascak P. B., Carlson R. W., and Shirey S. B. (1999) Accurate and precise determination of Li isotopic compositions by multi-collector sector ICP-MS. *Chemical Geology* **158**(1-2), 145-154.

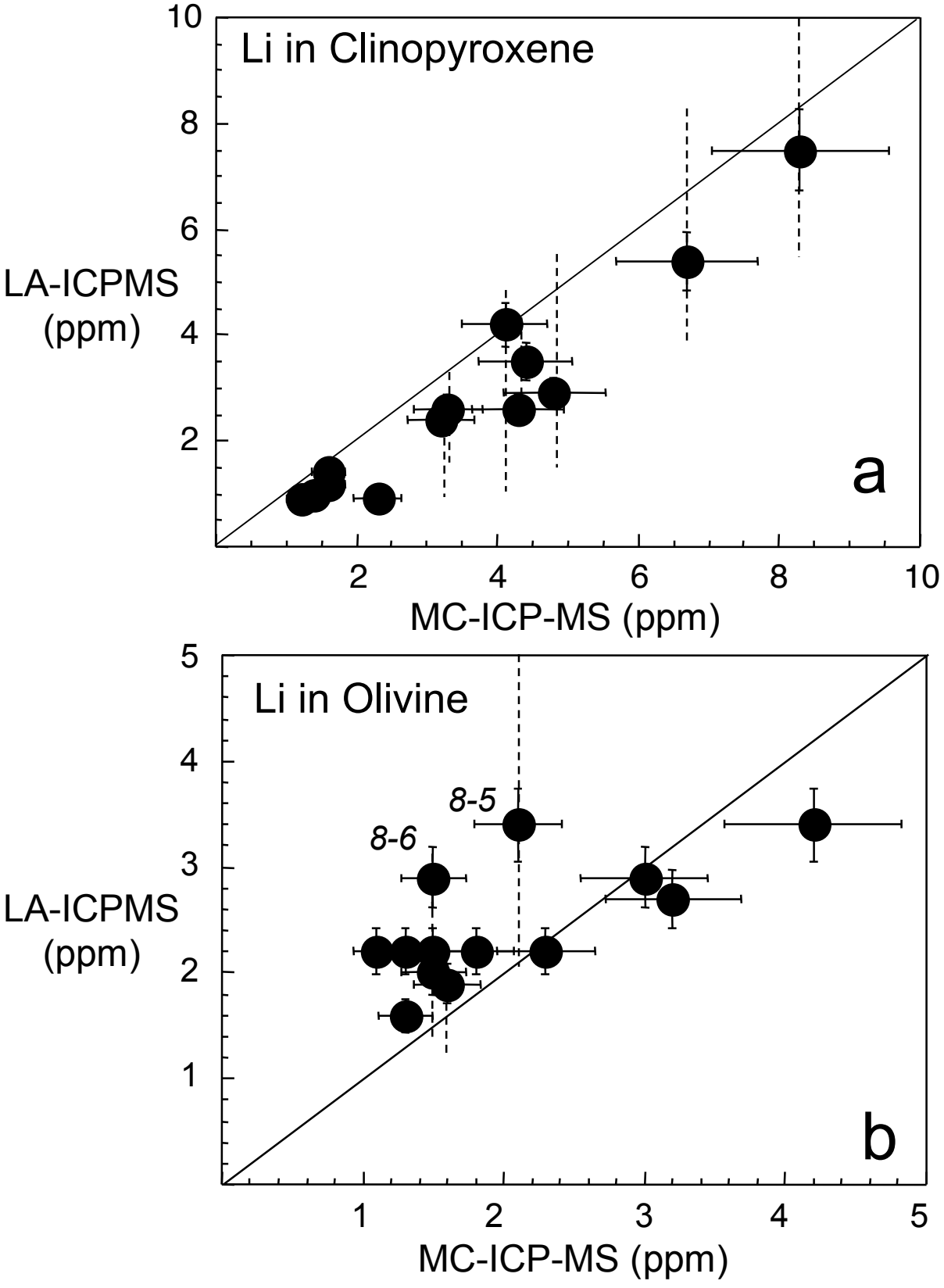
Li in Clinopyroxene
LA-ICPMS (ppm)
MC-ICP-MS (ppm)
a
Li in Olivine
8-5
8-6
LA-ICPMS (ppm)
MC-ICP-MS (ppm)
b

Figure S1

Electronic supplement

Figure S1. Comparison between Li concentrations determined on mineral solutions measured by multi-collector ICP-MS (MC-ICP-MS) and those determined *in situ* by laser ablation ICP-MS (LA-ICP-MS). A: cpx, B: olivine. Error bars represent ±15% for MC-ICP-MS and ±10% for LA-ICP-MS. Where multiple spots were analyzed by LA-ICP-MS, the range of values observed for individual spots are shown as a dotted line. In several cases the range is much larger than the analytical uncertainty, indicating heterogeneity of Li concentration. Olivine from sample 8-5 shows large variability in Li ppm between different grains.

Table S1. Lithium concentration profiles for minerals from selected Tok peridotite xenoliths

Sample	Position	Li ppm*	^{6}Li ppm	^{7}Li ppm
Lherzolites				
8-6 cpx-1	rim	5.31	5.34	5.27
	int. 1	4.26	4.44	4.09
	core	3.89	3.86	3.92
8-6 cpx-2	rim	9.63	10.08	9.18
	core	2.86	2.94	2.79
8-6 cpx-3	rim	6.11	6.27	5.95
	int. 1	3.91	4.06	3.76
	core	4.48	4.67	4.29
8-6 olivine-1	rim	2.24	2.30	2.17
	int. 1	3.12	3.28	2.95
	int. 2	3.05	2.99	3.11
	core	3.06	3.14	2.98
8-6 olivine-2	rim	3.75	3.88	3.63
	int. 1	3.56	3.73	3.38
	int. 2	3.31	3.47	3.16
	core	3.39	3.56	3.23
8-5 cpx	rim	5.70	5.76	5.64
	int. 1	4.22	4.33	4.12
	int. 2	3.45	3.47	3.43
	core	2.05	2.11	2.00
8-5 olivine	rim	2.52	2.22	2.20
	int. 1	2.59	2.21	2.40
	int. 2	2.50	2.38	2.47
	int. 3	2.42	2.47	2.54
	int. 4	2.31	2.64	2.53
	core	2.21	2.49	2.56
Harzburgite				
1-2 cpx-1	rim	4.91	4.98	4.83
	core	5.06	5.15	4.97
1-2 cpx-2	rim	4.25	4.34	4.16
	core	3.32	3.55	3.10
1-2 olivine	rim	4.13	4.20	4.06
	int. 1	4.23	4.34	4.13
	core	4.17	4.23	4.11

*Average of ppm values obtained using ^{7}Li and 6Li. Spot size: 120 μm